

ON THE INFLUENCE OF INCOMPLETE RADIATION PATTERN DATA ON THE ACCURACY OF A SPHERICAL WAVE EXPANSION

P. K. Koivisto and J. C.-E. Sten

VTT Information Technology, Telecommunications
P.O. Box 1202, FIN-02044 VTT, Finland

Abstract—The accuracy of a spherical wave expansion is examined when the expansion is calculated from incomplete data of the radiation pattern, i.e., when field data on a part of the far-field sphere is missing. The effect of antenna size and truncation index on the interpolation capacity of a SWE is examined by using an analytical expression for the radiation pattern of wire antennas of different lengths. The error of the SWE is seen to increase drastically when the smallest diameter of the dead zone surpasses the length of a period of the highest included wave function. The influence of the size and shape of the dead zone is studied by the aid of a measured pattern, of which a part of the field data is ignored. Two different ways are proposed for estimating the accuracy of the obtained SWE in a practical instance, when the field in the dead zone is unknown.

1 Introduction

2 Spherical Wave Expansion

2.1 Representation

2.2 Calculation of the Coefficients

3 Measurements and Calculations

3.1 Definition of the Dead Zone

3.2 Error of a Field

3.3 Used Field Data

4 Results

4.1 Effect of the Dead Zone on the Accuracy of the SWE

4.2 Estimation of the SWE Error without Knowledge of the Exact Field

5 Conclusions

References

1. INTRODUCTION

In some antenna radiation pattern measurement setups there exists a dead zone where, for some reason, data is not available. In such a case, if the dead zone is not too large, evaluation of a spherical wave expansion (SWE) can offer a means to recover a complete radiation pattern owing to the interpolation capacity of the SWE. This property and its limitations are studied in this paper in the light of examples involving small antennas.

A spherical wave expansion gives a truly three-dimensional representation of a radiation pattern. When the coefficients of the expansion are known, the electric and magnetic fields can be calculated everywhere outside the smallest origin centred sphere enclosing the antenna. Another benefit of the SWE is that merely by calculating the expansion with a proper truncation index one obtains a radiation pattern, which may be more accurate than the original (measured or simulated) data from which the expansion is calculated [1, 2].

This paper is organised as follows: In Section 2 the SWE and the technique for calculating its coefficients are introduced. Because of the presence of the dead zone, the expansion coefficients must be determined by matching the wave functions directly with measured fields instead of using the traditional orthogonality integrals. This leads to a rather large matrix equation, which, however, can be solved easily. The data used in the examples and the method used for calculating the error of a field are introduced in Section 3. Section 4 presents the obtained results. First, we study the effect of antenna size and truncation index on the accuracy of the SWE calculated from incomplete data generated by a theoretical formula. Second, the effect of the size and shape of the dead zone is examined using a realistic (measured) radiation pattern. In this connection, the influence of the error of the data itself is also taken into account. Examples of successful and failed SWEs are presented and, finally, two methods for estimating the accuracy of the calculated SWE without knowing the accurate field are introduced.

2. SPHERICAL WAVE EXPANSION

2.1. Representation

The SWE for the electric and magnetic fields outside the smallest possible origin centred sphere enclosing the source ($r > r_0$) is given by

$$\mathbf{E}(r, \theta, \phi) = \sum_{n=1}^{\infty} \sum_{m=-n}^n [a_{mn} \mathbf{M}_{mn}(r, \theta, \phi) + b_{mn} \mathbf{N}_{mn}(r, \theta, \phi)] \quad (1)$$

$$\mathbf{H}(r, \theta, \phi) = \frac{jk}{\omega\mu} \sum_{n=1}^{\infty} \sum_{m=-n}^n [b_{mn} \mathbf{M}_{mn}(r, \theta, \phi) + a_{mn} \mathbf{N}_{mn}(r, \theta, \phi)] \quad (2)$$

where $k = \omega\sqrt{\epsilon\mu} = 2\pi/\lambda$ is the wave number. Slightly different notations are used, e.g., in [3–6]. The vectors \mathbf{M}_{mn} and \mathbf{N}_{mn} , called vector spherical wave functions, are defined by

$$\begin{aligned} \mathbf{M}_{mn}(r, \theta, \phi) &= \nabla \times (\mathbf{r}\psi_{mn}) \\ \mathbf{N}_{mn}(r, \theta, \phi) &= k^{-1} \nabla \times \nabla \times (\mathbf{r}\psi_{mn}) \end{aligned} \quad (3)$$

where the scalar spherical wave functions for outward travelling fields are

$$\psi_{mn}(r, \theta, \phi) = e^{-jm\phi} h_n^{(2)}(kr) P_n^{|m|}(\cos \theta). \quad (4)$$

In these expressions, the functions $P_n^{|m|}$ are the associated Legendre functions and $h_n^{(2)}$ are the spherical Hankel functions of the second kind.

Using the asymptotic form of the spherical Hankel functions the electric field components in the far-field region can be expressed as

$$\begin{aligned} E_{\theta} &= \sum_{n=1}^{\infty} \sum_{m=-n}^n \left[a'_{mn}(-jm) \frac{P_n^{|m|}(\cos \theta)}{\sin \theta} + b'_{mn} \frac{dP_n^{|m|}(\cos \theta)}{d\theta} \right] \exp(-jm\phi) \\ E_{\phi} &= \sum_{n=1}^{\infty} \sum_{m=-n}^n \left[a'_{mn} \left(-\frac{dP_n^{|m|}(\cos \theta)}{d\theta} \right) + b'_{mn}(-jm) \frac{P_n^{|m|}(\cos \theta)}{\sin \theta} \right] \\ &\quad \times \exp(-jm\phi) \\ E_r &= 0 \end{aligned} \quad (5)$$

where

$$\begin{aligned} a'_{mn} &= a_{mn} h_n^{(2)}(kr) \approx j^{n+1} \frac{e^{-jkr}}{kr} a_{mn} \\ b'_{mn} &= b_{mn} \frac{1}{kr} \frac{d}{d(kr)} \left[h_n^{(2)}(kr) kr \right] \approx j^n \frac{e^{-jkr}}{kr} b_{mn} \end{aligned}$$

An accurate SWE contains, in principle, an infinite number of modes as shown by expressions (1), (2) and (5). In spite of this, a reasonably small number of lowest modes suffice in all practical problems, because the expansion, owing to the feature of spherical Hankel functions, converges rather quickly with increasing mode index for large mode indices. Thus, the SWE can be truncated at a relatively low mode index $n \leq N$ without a substantial error.

2.2. Calculation of the Coefficients

The classical method of obtaining the expansion coefficients [4] is based on the orthogonality of the complete base formed by the vector spherical wave functions \mathbf{M}_{mn} and \mathbf{N}_{mn} . The coefficients are obtained by integrating the dot product of the corresponding vector spherical wave function with the electric field over the entire sphere. Since the method requires that the electric field is known over the entire sphere containing the antenna the method cannot be applied with incomplete data. In this paper, a direct matching technique for obtaining the coefficients is applied instead of the classical orthogonality method. A similar technique was used in [7] for near-field data.

When the complex electric field in the far-field region is known, the complex coefficients of the SWE can be found by solving the set of linear equations given by the matrix equation

$$\mathbf{E} = \mathbf{M}\mathbf{A} \quad (6)$$

The vector \mathbf{E} consists of the complex electric field components in each measured directions

$$\mathbf{E} = [E_\theta(\theta_1, \phi_1)E_\theta(\theta_2, \phi_2) \cdots E_\theta(\theta_M, \phi_M)E_\phi(\theta_1, \phi_1)E_\phi(\theta_2, \phi_2) \cdots E_\phi(\theta_M, \phi_M)]^T \quad (7)$$

where M is the total number of measurement directions. The vector \mathbf{A} consists of the complex coefficients of the SWE truncated at the mode index $n = N$

$$\begin{aligned} \mathbf{A} &= [(a_{-1,1}c_{-1,1}) (a_{0,1}c_{0,1}) (a_{1,1}c_{1,1}) (a_{-2,2}c_{-2,2}) \\ &\quad \cdots (a_{N,N}c_{N,N}) (b_{-1,1}c_{-1,1}) \cdots (b_{N,N}c_{N,N})]^T \quad (8) \\ c_{mn} &= \sqrt{\frac{2n(n+1)}{2n+1} \frac{(n+|m|)!}{(n-|m|)!}} \end{aligned}$$

The matrix \mathbf{M} is

$$\mathbf{M} = \begin{pmatrix} \mathbf{F} & \mathbf{G} \\ -\mathbf{G} & \mathbf{F} \end{pmatrix} \quad (9)$$

where

$$\mathbf{F} = \begin{pmatrix} f_{-1,1}(\theta_1, \phi_1) & \cdots & f_{N,N}(\theta_1, \phi_1) \\ \vdots & \ddots & \vdots \\ f_{-1,1}(\theta_M, \phi_M) & \cdots & f_{N,N}(\theta_M, \phi_M) \end{pmatrix}$$

$$\mathbf{G} = \begin{pmatrix} g_{-1,1}(\theta_1, \phi_1) & \cdots & g_{N,N}(\theta_1, \phi_1) \\ \vdots & \ddots & \vdots \\ g_{-1,1}(\theta_M, \phi_M) & \cdots & g_{N,N}(\theta_M, \phi_M) \end{pmatrix}$$

$$f_{m,n}(\theta, \phi) = -jm \frac{P_n^{|m|}(\cos \theta) e^{-jm\phi}}{\sin \theta c_{m,n}}$$

$$g_{m,n}(\theta, \phi) = \frac{dP_n^{|m|}(\cos \theta) e^{-jm\phi}}{d\theta c_{m,n}}$$

In order to get unique solution, the set of Equations (6) must not be underdetermined, meaning that the length of \mathbf{E} should be equal to or larger than the length of \mathbf{A} . It thus follows that the number of data points M must fulfil the condition $M \geq N(N + 2)$. In Matlab, which is used in all calculations in this paper, the solution is found easily by the matrix “left division” ($\mathbf{A} = \mathbf{M} \setminus \mathbf{E}$), which operation finds the least squares solution to the overdetermined set of Equations (6).

3. MEASUREMENTS AND CALCULATIONS

3.1. Definition of the Dead Zone

The incomplete data is produced from the complete radiation pattern simply by omitting the data in the dead zone area. We define the dead zone here through the angles θ' , ϕ' , α and β , where the direction $(\theta, \phi) = (\theta', \phi')$ represents the centre of the dead zone while the angles α and β determine its size and shape. The shape is determined in the special case of $(\theta', \phi') = (90^\circ, \phi')$, in which case the dead zone covers the directions $\phi' - \beta \leq \phi \leq \phi' + \beta$ and $90^\circ - \alpha \leq \theta \leq 90^\circ + \alpha$. In other cases, the defined dead zone is rotated so that its shape remains the same and the centre point lies in the desired direction. An example of a dead zone and included data directions is shown in Figure 1, where $\theta' = 90^\circ$ and $\phi' = 0^\circ$.

The size of the dead zone can be measured by the fraction of the

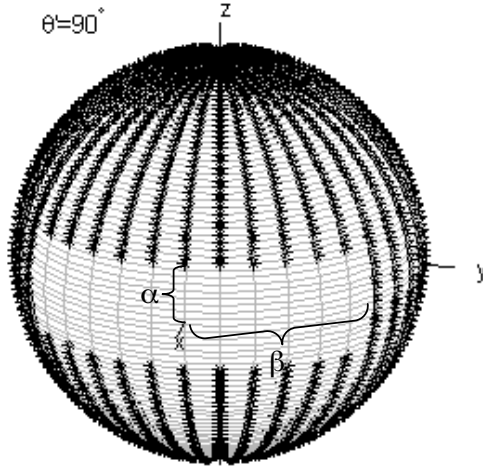


Figure 1. Example illustrating incomplete data. Directions of the included data points are marked with asterisks.

dead zone area from the area of the whole sphere, given by

$$\Omega = \frac{\int_{\frac{\pi}{2}-\alpha}^{\frac{\pi}{2}+\alpha} \int_{-\beta}^{\beta} \sin \theta d\phi d\theta}{4\pi} = \frac{\beta \sin \alpha}{\pi} 100\% \quad (10)$$

3.2. Error of a Field

By the difference of two fields, Δ_E , we mean the rms. difference between the reference field (E^{ref}) and the field under study (E) normalised by the average amplitude of the reference field. The difference is expressed by the formula

$$\Delta_E = \left[\frac{1}{M} \sum_{k=1}^M \left\{ \left| E_{\theta k}^{ref} - E_{\theta k} \right|^2 + \left| E_{\phi k}^{ref} - E_{\phi k} \right|^2 \right\} / \left(\tilde{E}^{ref} \right)^2 \right]^{1/2} \quad (11)$$

where the index k runs through all the M directions where the field components are known and the average amplitude of the reference field is calculated as

$$\left(\tilde{E}^{ref} \right)^2 = \frac{1}{4\pi} \int_0^{\pi} \int_0^{2\pi} \left(\left| E_{\theta}^{ref}(\theta, \phi) \right|^2 + \left| E_{\phi}^{ref}(\theta, \phi) \right|^2 \right) \sin \theta d\phi d\theta$$

The error of a field is defined as the smallest possible difference from the corresponding exact reference field, that is,

$$\delta_E = \min \{ \Delta_E \} \quad (12)$$

The minimum is sought from all possible combinations of position, alignment, constant phase and power of the field under study. This procedure ensures that the considered expansion is expressed in the same co-ordinates as the reference field, that the fields are cophasal and that they contain the same amount of power. In practice, the minimisation is carried out as follows. First, a position is sought for the expansion centre, with which the power is in as low a mode number n as possible, for both the considered and the exact field. Then the difference is further minimised by varying the position, alignment, power, and constant phase of the measured field. For this, an appropriate phase and position are found roughly by a genetic algorithm, which result is further improved by means of the Nelder-Mead method included in Matlab. Finally, the Nelder-Mead method is applied again to find a proper rotation and power.

3.3. Used Field Data

The effect of incomplete data is studied with both a theoretical and a measured radiation pattern. First, an analytical expression for the radiation pattern of a linear wire antenna is used to study the interpolation capacity of the SWE as a function of antenna size and truncation index. The omnidirectional radiation pattern of a linear wire dipole of length $2l$, placed along the z -axis is

$$E_\theta \propto \frac{\cos(kl \cos \theta) - \cos(kl)}{\sin \theta} \quad (13)$$

The complete data contains the fields given by (13) in cuts $\phi = 0^\circ, 10^\circ \dots 170^\circ$ with $\theta = -177^\circ, -175^\circ, \dots 177^\circ$. While calculating the error, the analytical expression (13) is used as the exact reference field. Because the same formula is used to generate the data and the reference field, the equality of co-ordinates and power as well as the cophasality are guaranteed. Thus, the minimising process is not necessary in this case. Since the data used is exact, the error of the SWE calculated from the complete data arises only from the truncation of the expansion. Exclusion of the data in the dead zone increases the error of the obtained SWE.

In the second example, the interpolation with SWE is studied using a measured radiation pattern. The antenna considered as an example consists of a monopole (length 38 mm) on a metal box

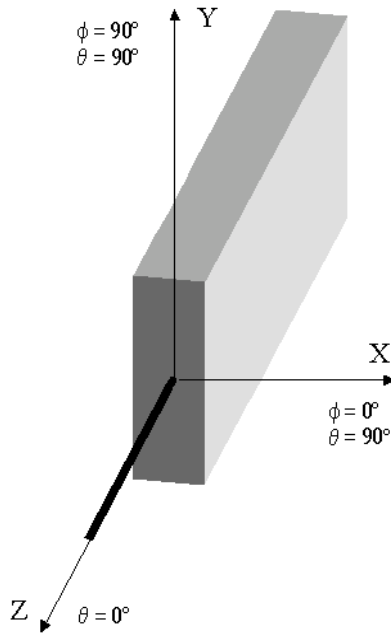


Figure 2. A sketch of the geometry of the measured antenna placed in the used co-ordinates.

(size: $100 \text{ mm} \times 40 \text{ mm} \times 16 \text{ mm}$), the geometry of which is shown in Figure 2. In the chosen co-ordinates the electrical size $kr_0 = 4.29$, where r_0 is the radius of smallest origin centered sphere enclosing the antenna. The complete radiation pattern was measured at the frequency 2 GHz in 18 cuts ($\phi = 0^\circ, 10^\circ \dots 170^\circ$) with 176 θ -values ($\theta = -175^\circ, -173^\circ \dots 175^\circ$), which yield $M = 3168$ measured directions. The number is clearly larger than required by the size of the antenna, thus assuring that the sparseness of the measurement directions does not affect the accuracy of the obtained SWE.

In order to have the reference, or “exact”, field in (12), the radiation pattern was calculated using the IE3D simulator at the same frequency and in the same directions as the measurement was carried out. Now the minimising process is necessary because the correspondence of the measured and simulated field is not guaranteed automatically. In this case, the error of the SWE calculated from the complete data arises mostly from the inaccuracy of the measured data, while the part of error caused by the truncation is negligible.

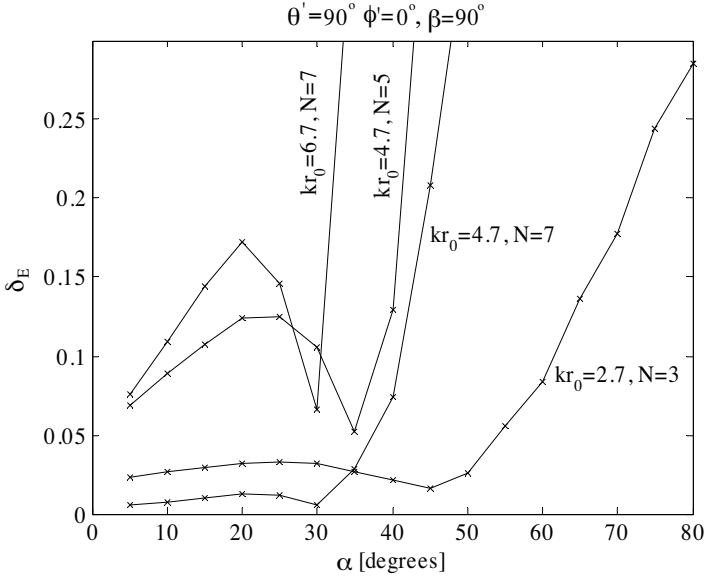


Figure 3. Error of the SWEs calculated from incomplete data of wire antennas with different length. The electrical size kr_0 and the truncation index N are given in the figure.

4. RESULTS

4.1. Effect of the Dead Zone on the Accuracy of the SWE

The effect of the dead zone on the accuracy of the obtained SWE is conveniently studied if the exact field is known. First, let us consider the linear wire dipole with the radiation pattern (13). The error of the SWE obtained from this pattern using different truncation indices is evaluated for different α of the dead zone, when $\beta = 90^\circ$, $\theta' = 90^\circ$ and $\phi' = 0^\circ$. As seen in Figure 3, the error of the SWE increases rapidly beyond a certain α , which we adopt as the limit for an acceptable accuracy of the SWE. The calculations show that the allowable dead zone width depends mostly on the used truncation index, which in turn is chosen according to the antenna size. Generally, the truncation index N should be at least of the order of kr_0 , but choosing N larger than this leads to a better accuracy. However, with an increasing N the width of the dead zone leading to an acceptable SWE becomes narrower due to a growing spatial frequency of the spherical wave functions of growing order. A wave function of order n can manifest $n/2$ periods in a span of 180° , thus giving $360^\circ/n$ as the approximate width of one such period.

The examples of Figure 3 confirm that the limiting α is approximately equal to $180^\circ/N$. This result means that the SWE can interpolate the radiation pattern over a large dead zone successfully when the antenna is reasonably small in terms of wavelengths. With electrically large antennas, only very narrow dead zones can be covered with a SWE.

Now let us consider a measured data obtained as explained in Section 3.3. For this data, SWEs were calculated from incomplete data with several different sizes and shapes and two different centres of the dead zone. The calculations were carried out with $\beta = 25^\circ, 55^\circ, 85^\circ, 115^\circ$ and $\alpha = 5^\circ, 10^\circ, 15^\circ \dots 90^\circ$ (see Figure 1). Furthermore, two directions for the centre point of the dead zone were considered: $\theta' = 90^\circ, \phi' = 0^\circ$ and $\theta' = 130^\circ, \phi' = 0^\circ$. In both cases, the shape of the region remained the same. An example of both cases are drawn in Figure 4, which shows that the direction $\theta' = 130^\circ$ lays in the high field intensity region, while the direction $\theta' = 90^\circ$ is situated in the low intensity region. Of course, when $\alpha \geq 40^\circ$ the dead zone covers both regions. In all calculations the expansion was truncated at $N = 6$.

Figure 5 and Figure 6 show the errors of the SWEs calculated from incomplete data as a function of the dead zone area (10) for the two positions of the dead zone, respectively. Two different data accuracies were used, as represented in case a) and b), respectively. The less accurate data (error $\delta_E^d = 0.1793$) is the original measured data, while the more accurate data (error $\delta_E^d = 0.0621$) was obtained from the original data by eliminating the rotation axis offset as explained in [8].

In all cases, when the dead zone area is less than 15% of the whole sphere, the error of the SWE field is smaller than the data error (the horizontal line in the figures). When the dead zone area is larger than 30%, the error of the SWE always exceeds the data error and the expansion fails.

It can be seen that not only the area of the dead zone but also its shape have an effect on the accuracy of the SWE. For a narrow dead zone the SWE might be more accurate than for a square-like dead zone with a smaller area. For the particular field studied here, the accuracy of the SWE is better than the accuracy of the data when $\alpha \leq 20^\circ$ or $\beta \leq 25^\circ$, which agrees with the rule for the maximum width of the dead zone given above.

The error of the SWE field also depends on the accuracy of the data. From the examples considered in Figures 5 and 6 one may conclude that, with small dead zone areas ($\Omega < 20\%$), where the error of the SWE field is reasonably small, the error of the SWE field relative to the data error is almost unchanged for similar size, shape

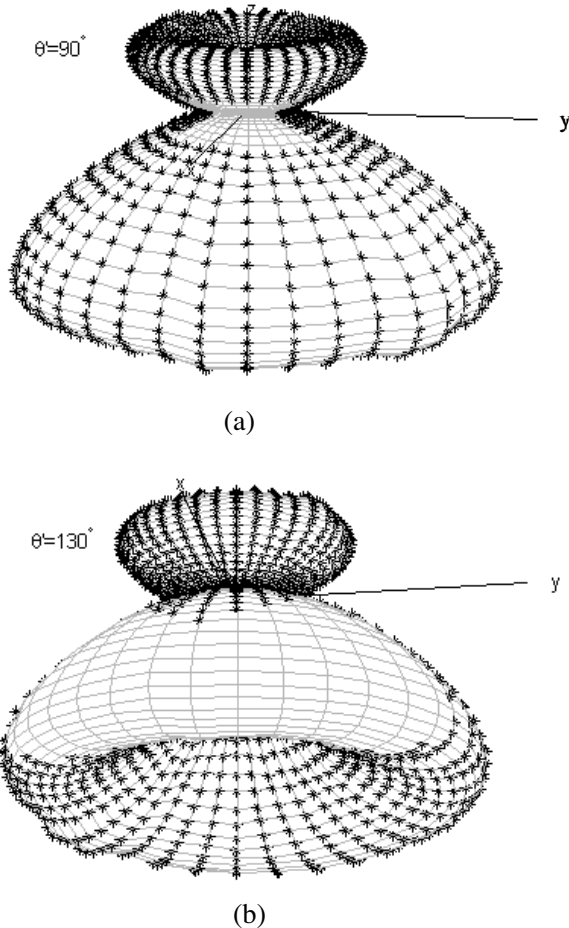
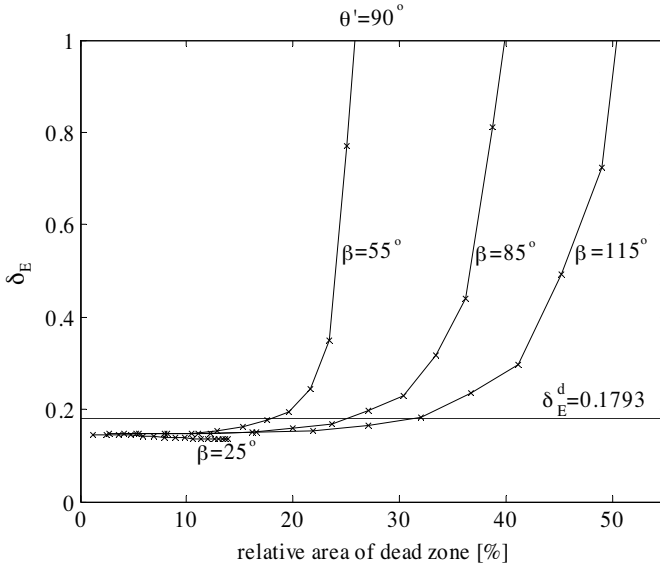


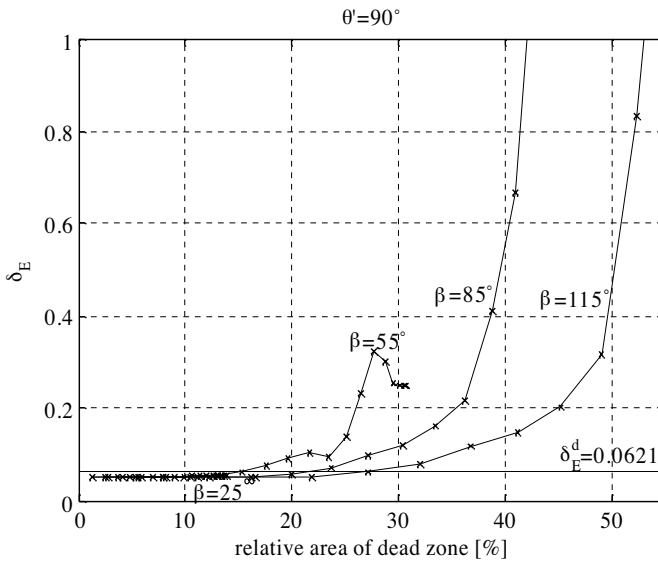
Figure 4. The measured radiation pattern (proportional to the total power) of the antenna with the directions of the included data marked with asterisks for the two dead zone positions used. In both examples $\alpha = 15^\circ$ and $\beta = 55^\circ$.

and position of the dead zone. With large dead zone areas, on the other hand, the exact amount of error is irrelevant because the error prevents the modelling of the radiation pattern. It can also be seen, that the position of the dead zone has no significant effect on the achieved accuracy of the SWE.

In the following, examples of a successful ($\delta_E = 0.0537$) and a failed ($\delta_E = 0.3219$) SWE calculation are presented. In both cases the

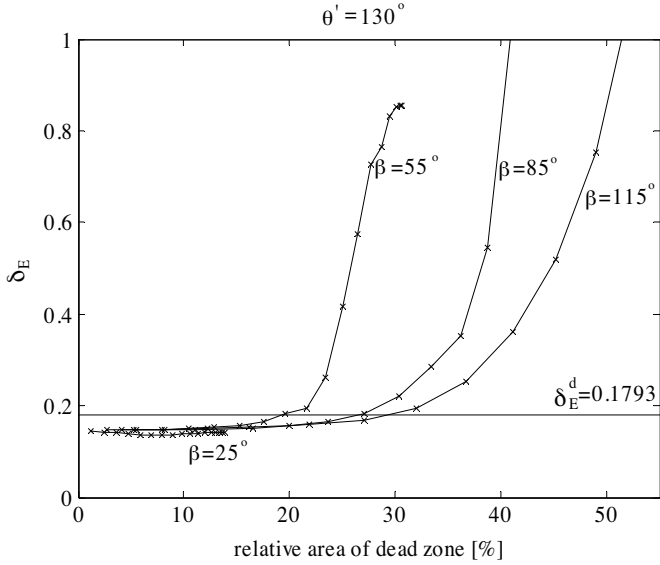


(a)

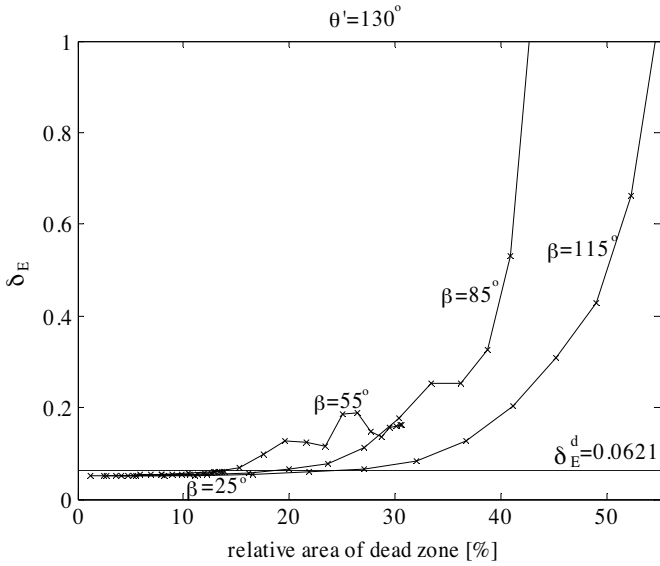


(b)

Figure 5. Error of the SWE calculated from incomplete data as a function of dead zone area. The dead zone lies in the low intensity region ($\theta' = 90^\circ$, $\phi' = 0^\circ$, see Figure 4a).



(a)



(b)

Figure 6. Same as Figure 5. The dead zone lies in the high intensity region ($\theta' = 130^\circ$, $\phi' = 0^\circ$, see Figure 4b).

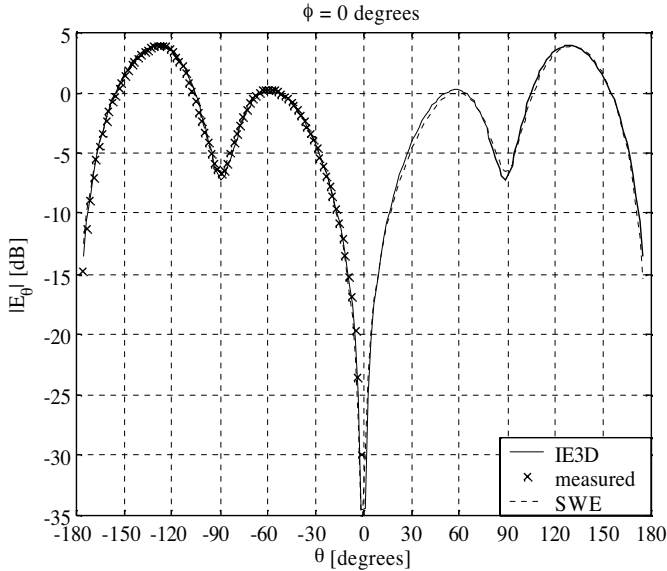


Figure 7. Amplitude of the E_θ component in the $\phi = 0^\circ$ cut, when the data error is $\delta_E^d = 0.0621$ and $\alpha = 90^\circ$ and $\beta = 25^\circ$ (corresponding to $\Omega = 14\%$).

data error is $\delta_E^d = 0.0621$, and the dead zone direction is $\theta' = 90^\circ$, $\phi' = 0^\circ$. Figure 7 shows the amplitude of electric field θ -component, when the dead zone dimensions are $\alpha = 90^\circ$, $\beta = 25^\circ$ (the dead zone area is 14%). In spite of the large α -value, the agreement of the SWE and simulated fields is good, because the dead zone is narrow enough. An example of a failed SWE calculation is demonstrated in Figure 8 when the dead zone dimensions are $\alpha = 65^\circ$ and $\beta = 55^\circ$ (the dead zone area is 28%). Now, the disagreement in the dead zone is obvious. The 3D radiation patterns proportional to the total power for the calculated SWE in the two cases can be seen in Figure 9. The agreements and disagreements of the two patterns are seen clearly by comparing them with the measured radiation pattern in Figure 4.

4.2. Estimation of the SWE Error without Knowledge of the Exact Field

In practical situations, there is no exact data available with which to check the validity of the SWE recovered from the incomplete data. Thus, in the following we present two methods that can be used to assess the validity of a SWE.

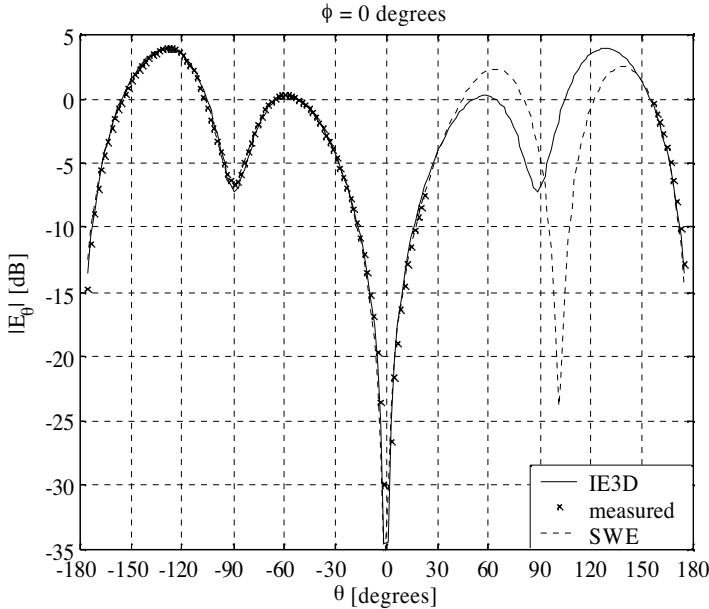


Figure 8. Same as Figure 7, when $\alpha = 65^\circ$ and $\beta = 55^\circ$ (corresponding to $\Omega = 28\%$).

The first crude method is based on a comparison of the power content of the original field and that of the SWE. The method is based on the property illustrated in the following example. Suppose we model the spherical harmonic mode $n = 7, m = 2$ by an expansion which is truncated at $N = 6$. Figure 10 shows the power distribution as a function of mode index n for the complete data and for the incomplete data, with the two dead zone sizes discussed in the previous Section. Besides shifting to low order modes, the power included into the expansion can be seen to increase when the size of the dead zone grows. When the dead zone is the largest the power in the modes $n = 1 - 6$ exceeds considerably the power of the original $n = 7$ mode. In fact, even for the complete data, the calculated expansion contains about one tenth of the power of the original mode, even if it should be zero by theory. Thus, we have demonstrated that the modes with mode indices higher than those taken into the SWE are not properly filtered out of the expansion, as they would be if the dead zone were small enough.

The tendency towards increasing power in the truncated SWE due to the excluded modes offers a means to check the validity of

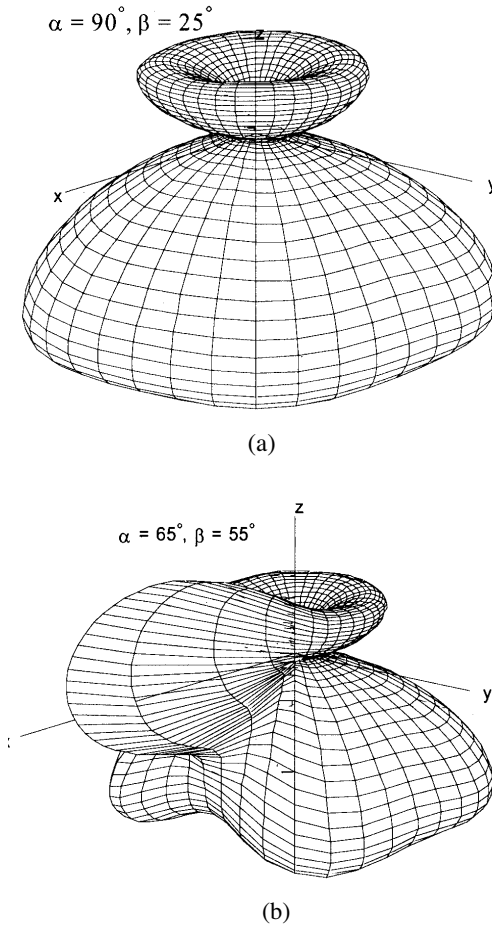


Figure 9. Radiation patterns proportional to total power for two different dead zone sizes. The middle point of the dead zone is in the direction $\theta' = 90^\circ$, $\phi' = 0^\circ$ and the data error is $\delta_{E}^d = 0.0621$ in both cases.

the calculated expansion, when the radiated power of the measured antenna is approximately known. If the power of the calculated SWE field exceeds the expected value considerably, one can be sure that the expansion fails to model the measured field. However, this method is not reliable, because the power of the SWE field can be low even though the expansion is inaccurate.

The second refined method is based on a comparison of the fields

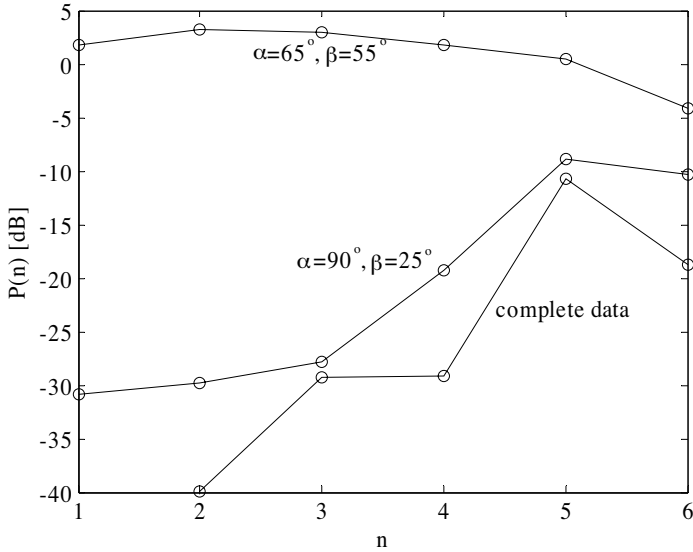


Figure 10. Modelling the mode $n = 7, m = 2, \alpha'_{27} = 0.00941154$ (power $P = 0$ dB) with an expansion of modes $1 \leq n \leq 6$. Power distribution as a function of mode index n .

of two different SWEs, obtained from two randomly selected subsets of the original data. The difference of the two fields is calculated using formula (11) separately for the dead zone ($\Delta_E(\text{dead zone})$) and for the region where the data is known ($\Delta_E(\text{data})$). It is observed that both the error and the difference of the two fields increase in the dead zone, while the area of the zone is growing. In the known data region, nevertheless, the difference decreases because the number of the data decreases. Thus, it is useful to study the ratio of the differences in the dead zone and in the data region. This ratio is drawn in Figure 11 as a function of the dead zone area in the case of the two data accuracies. Comparison of Figure 11a) with Figure 5a) (data error $\delta_E^d = 0.1793$) and Figure 11b) with Figure 5 b) (data error $\delta_E^d = 0.0621$), tells that the error of the SWE exceeds the data error when the ratio goes above 5 to 12 and 5, respectively. These ratios can, in the present examples, be considered as the upper limits for a successful recovery of the SWE.

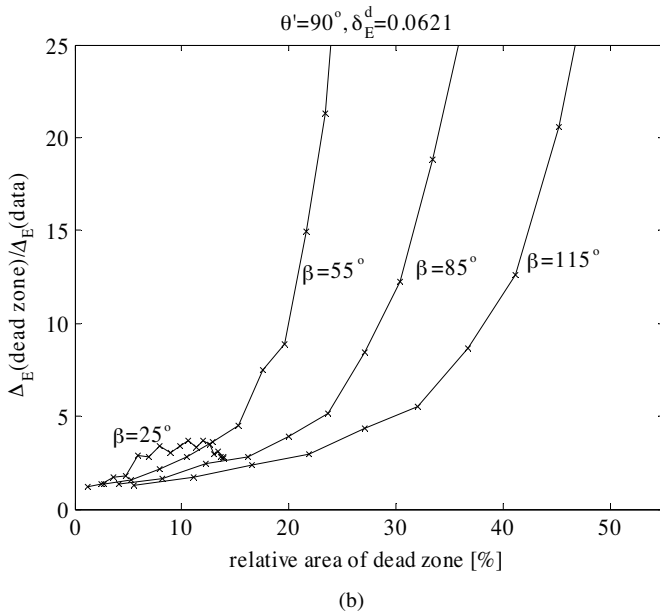
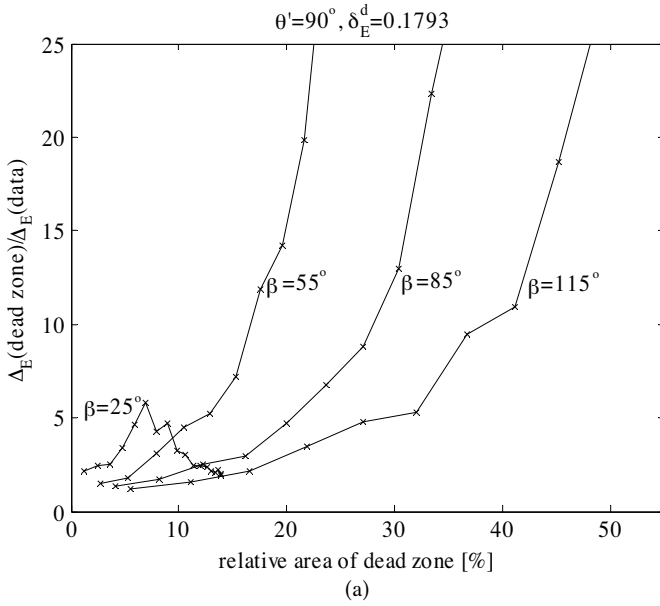


Figure 11. Ratio of the SWE field differences for dead zone and known data region. The data error is $\delta_E = 0.1793$ in case a) and $\delta_E = 0.0621$ in case b).

5. CONCLUSIONS

The effects of the incompleteness of data on the accuracy of a SWE have been examined using analytical, measured and simulated radiation patterns. It was found that a successful interpolation of the field in the dead zone requires that the smaller diameter of the dead zone shall not be greater than a certain value determined by the truncation index of the expansion, which in turn is a function of the electrical size of the antenna and the required accuracy. This value for the smallest dimension was found to be roughly one period of the highest included wave function. If the dead zone diameter is larger than this limit the error of the expansion increases drastically.

Both the size and the shape of the dead zone have an effect on the accuracy. It was found that the SWE might be more accurate for a narrow dead zone than for a square-like dead zone with smaller area. The error of the field for the calculated expansion is also dependent on the accuracy of the data. With the measured radiation pattern considered in this paper, the error of the SWE field relative to the data error used is almost independent of the data accuracy. Two means have been discussed for estimating whether the expansion is successful or not without knowledge of the exact radiation pattern. With a growing dead zone area, the total power of the SWE tends to increase together with the error. If the power of the calculated SWE exceeds the expected value noticeably, one can be sure that the expansion has failed. On the other hand, one cannot be sure that the SWE is accurate if the power of the SWE has the expected value. As another means to determine the accuracy of the SWE, we considered the rms. difference of two expansions, obtained from two sets of data selected randomly from the available incomplete data. The ratio between this rms. difference in the dead zone and in the data region is seen to increase with an increasing error of the expansion. It would be worthwhile to examine further these two and other possible techniques to obtain a reliable way to estimate the accuracy of the obtained SWE.

REFERENCES

1. Koivisto, P., "Reduction of errors in antenna radiation patterns using optimally truncated spherical wave expansion," *Progress In Electromagnetics Research (PIER)*, Vol. 47, 313–333, 2004.
2. Koivisto, P., "Demonstration of reflection error reduction in antenna radiation patterns using spherical wave expansion," *Microwave and Optical Technology Letters*, November 20, 2004.
3. Hansen, J. E. (Ed.), *Spherical Near-Field Antenna Measurements*,

- IEE Electromagnetic Waves Series 26, Peter Peregrinus Ltd., London, United Kingdom, 1988.
4. Harrington, R. F., *Time-Harmonic Electromagnetic Fields*, McGraw-Hill, 1961.
 5. Stratton, J. A., *Electromagnetic Theory*, 1st Ed., McGraw-Hill, New York and London, 1941.
 6. Papas, C. H., *Theory of Electromagnetic Wave Propagation*, Dover Publications, Inc., New York, 1988.
 7. Mekki-Kaidi, M., D. Lautru, F. Bancet, and V. Fouad Hanna, "A matrix inversion technique for the spherical modal decomposition field solution applied on the characterization of antennas in their environment," *Microwave and Optical Technology Letters*, Vol. 41, No. 5, 336–341, June 2004.
 8. Koivisto, P., "Elimination of rotation axes offset error in antenna radiation pattern measurements using spherical wave expansion," Submitted for publication in *Int. J. Electron. Commun. (AEü)*.

Päivi K. Koivisto received the degrees of Dipl.Eng., Lic.Tech. and Dr.Tech. from the Helsinki University of Technology in 1985, 1992 and 1994, respectively. Presently she is with the VTT Information Technology. Her interest range from antennas to numerical and analytical electromagnetics.

Johan Carl-Erik Sten, was born in Helsingfors, Finland, in 1967. He received the degree of teknologie doktor in electrical engineering from Helsinki University of Technology (HUT) in 1995. From 1991 to 1994 he was with the Laboratory of Electromagnetics of HUT and from 1995 onward with VTT Information Technology. Presently his research focuses especially on the role of minimum-energy and nonradiating sources in antenna design.